Article:

Dong, Z, Meng, J, Zhu, H et al. (5 more authors) (2017) Synthesis of SiC nanowires via catalyst-free pyrolysis of silicon-containing carbon materials derived from a hybrid precursor. Ceramics International, 43 (14). pp. 11006-11014. ISSN 0272-8842

https://doi.org/10.1016/j.ceramint.2017.05.142

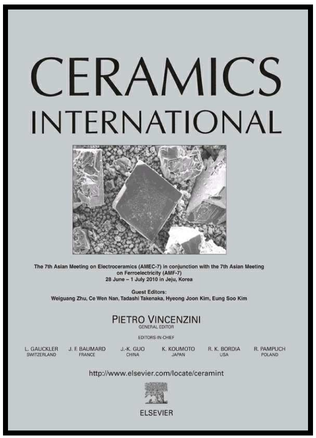

www.elsevier.com/locate/ceri

Synthesis of SiC nanowires via catalyst-free pyrolysis of silicon-containing carbon materials derived from a hybrid precursor

Zhijun Dong, Jian Meng, Hui Zhu, Guanming Yuan, Ye Cong, Jiang Zhang, Xuanke Li, Aidan Westwood

PII: S0272-8842(17)30954-9
DOI: http://dx.doi.org/10.1016/j.ceramint.2017.05.142
Reference: CERI15302

To appear in: *Ceramics International*

Received date: 3 January 2017
Revised date: 15 May 2017
Accepted date: 19 May 2017

Cite this article as: Zhijun Dong, Jian Meng, Hui Zhu, Guanming Yuan, Ye Cong, Jiang Zhang, Xuanke Li and Aidan Westwood, Synthesis of SiC nanowires via catalyst-free pyrolysis of silicon-containing carbon material derived from a hybrid precursor, *Ceramics Internationa* http://dx.doi.org/10.1016/j.ceramint.2017.05.142

Synthesis of SiC nanowires via catalyst-free pyrolysis of silicon-containing carbon materials derived from a hybrid precursor

Zhijun Dong[a, b], Jian Meng[b], Hui Zhu[b], Guanming Yuan[a, b], Ye Cong[a, b], Jiang Zhang [b], Xuanke Li [a,b,c*], Aidan Westwood[d]

[a] The State Key Laboratory of Refractories and Metallurgy, Wuhan University of Science and Technology, Wuhan, Hubei 430081, PR China

[b] The Hubei Province Key Laboratory of Coal Conversion & New Carbon Materials, Wuhan University of Science and Technology, Wuhan, Hubei 430081, PR China

[c] The research center for advanced carbon materials, Hunan University, Changsha, Hunan 410082, P. R. China

[d] School of Chemical and Process Engineering, University of Leeds, Leeds, LS2 9JT, U.K.

*Corresponding author. Tel/ Fax: +86 27 86556906. E-mail address: xkli@21cn.com (X.K. Li)

Abstract

SiC nanowires were successfully synthesized without catalyst by pyrolysis of silicon-containing pitch-derived carbon materials in a closed graphite crucible. These silicon-containing carbon materials were obtained by homogenization and co-carbonization of a hybrid precursor consisting of the toluene soluble fraction of coal tar pitch with polycarbosilane (PCS). The composition, morphology and structure of the nanowires were characterized by X-ray diffraction (XRD), scanning electron microscopy (SEM), transmission electron microscopy (TEM) and selected area electron diffraction (SAED). The influence of pyrolysis temperature on the growth of the nanowires was investigated by Fourier transform infrared spectroscopy (FTIR) and thermo-gravimetry coupled with mass spectroscopy (TG-MS) analysis. The results indicate that the growth of the SiC nanowires starts at around 1200 °C. As the pyrolysis temperature increases to 1300-1500 °C, a large quantity of nanowires are formed on the top surface of the pitch-derived carbon substrate. In addition, increasing the pyrolysis temperature leads to an increase in the average diameter and a change in the typical morphology produced. The synthesized SiC nanowires have single-crystalline structure and are grown along the [111] direction with numerous stacking faults and twins. The vapor-solid (VS) mechanism may be responsible for the growth process of the SiC nanowires.

Key words: SiC nanowires; hybrid precursor; pyrolysis; pitch-derived carbon materials

1. Introduction

Over the past decades, one-dimensional (1D) silicon carbide (SiC) nanowires have attracted considerable attention due to their unique characteristics, such as high thermal stability, excellent oxidation resistance, wide energy band gap, outstanding mechanical strength and excellent electromagnetic interference shielding performance. These properties make SiC nanowires a promising candidate material for many applications, such as reinforcement material, catalysis supports, panel displays, electronic and optoelectronic nanodevices, etc. [1-3]. Thus, many efforts have been devoted to the synthesis of SiC nanowires.

Up to now, various synthesis methods have been developed including carbo-thermal reduction [4], carbon nanotube template conversion [5], catalyst assisted chemical vapor deposition [6], solvothermal method [7], etc. Nevertheless, these methods are time-consuming and are often associated with low yield. In particular, the control of composition, dimensions and morphology of the resulting nanowires cannot be achieved easily by the above methods. These shortcomings limit their further application. Recently, polymer precursor pyrolysis has been developed for the synthesis of SiC nanowires from preceramic polymers including polysilazane, polycarbosilanes (PCS), polysilacarbosilane and hexamethyldisilane [8-11]. This process has demonstrated advantages of simplicity and easy control of the composition, dimensions and morphology of the resulting nanowires. Unfortunately, only a low yield of SiC nanowires can be obtained by catalyst-free polymer precursor pyrolysis. In order to increase the yield of SiC nanowires, a transition metal catalyst (Fe, Ni, Co, Cr, etc.) is usually introduced into the polymer precursor to facilitate the nucleation and growth of SiC nanowires [12, 13]. However, it is always very difficult to remove the residual metal catalyst from the SiC nanowires and it acts as an impurity, resulting in the degradation in their electronic and mechanical properties under harsh environmental conditions. Therefore, it is necessary to develop an efficient method to synthesize metal-free SiC nanowires on a large scale for further practical applications.

In this work, a simple and convenient method is put forward for synthesis of a large quantity of SiC nanowires via catalyst-free pyrolysis of silicon-containing carbon materials, which are obtained by homogenization and co-carbonization of a hybrid precursor consisting of the toluene soluble fraction of coal tar pitch and polycarbosilane (PCS). The effect of pyrolysis temperature on the phase composition, morphology and microstructure of the resulting nanowires is discussed. A tentative growth model, based on the vapor-solid (VS) mechanism, is also proposed to explain the growth of the SiC nanowires.

2. Experimental details

2.1 Starting raw materials

Coal tar pitch was a generous gift from Jining Carbon Group Co., Ltd (Jining, China) and was used as a carbon source. PCS was provided by Cerafil Ceramic Fiber Co., Ltd (Suzhou, China) and was utilized as a silicon source. The main properties of the coal tar pitch and PCS are listed in Table 1 and Table 2, respectively. Aldrich Chemical Co. supplied toluene, which was used as solvent without further purification.

2.2 Synthesis procedure

To ensure homogeneous mixing of the pitch and PCS in toluene, the toluene soluble fraction was separated from the coal tar pitch by solvent extraction and vacuum distillation. Toluene-soluble coal tar pitch (TSCTP) and PCS with a weight ratio of 1:1 were dissolved in toluene and mixed well via ultrasonic vibration. Then, the mixture was poured into a stainless steel reactor and heated at 350 °C under a protective argon atmosphere for 4 h, during which the mixture was homogenized. The apparatus was then allowed to cool down naturally and the homogenized mixture (a dark shiny solid) of TSCTP and PCS resulted. The homogenized mixture was further carbonized at 900 °C for 2 h under a protective argon atmosphere to remove the low boiling point fraction. The carbonized product was then ground into fine powder. Thereafter, the powder was immersed in 2M HCl solution for 48 h to remove the iron oxide contamination that arose from the stainless steel reactor. After drying at 100 °C for 1 h, the powder was pressed into disc-shaped samples with a diameter of 20 mm and thickness of 3 mm under 130 MPa pressure using a stainless steel die. The disc-shaped samples, namely silicon-containing pitch-derived carbon materials, were placed in a high-purity graphite crucible sealed with a lid and pyrolyzed at various temperatures (1200 °C, 1300 °C, 1400°C and 1500 °C) for 1 h in a vertical graphite furnace. After the furnace was allowed to cool naturally to room temperature, the graphite crucible was taken out. A large quantity of nanowires are formed on the top surface of the disc-shaped samples when the pyrolysis temperature is over 1200 °C. They were easily collected by brushing them from the sample surface.

2.3 Characterization

The phase composition of the samples was identified by an X-ray diffraction (XRD) instrument (Philips X'Pert Pro MPD) using Cu-K_α radiation (λ=1.54056 Å). The working voltage and current of the Cu target were 40 kV and 40 mA, respectively. A field emission scanning electron microscope (FESEM, NOVA400 NANOSEM) was used to observe the morphology of the samples. The elemental composition of the samples was analyzed by an energy-dispersive X-ray spectroscopy (EDX) attached to the abovementioned FESEM. A high resolution transmission electron microscope (HR-TEM Model JEM-2010 UHR JEOL, Japan) was employed to further characterize the microstructure of the samples. This was equipped with an energy dispersion spectroscopy attachment (EDSINCA IE 350 Penta FET X-3, Oxford, UK) and operated at 300 kV. For HRTEM and SAED observations, the nanowire sample was firstly dispersed in an alcohol solution via ultrasonic vibration. The alcohol containing nanowires was then dropped onto a copper grid, and naturally dried before analysis. On-line TG–MS analyses of the gases evolved from the silicon-containing pitch-derived carbon materials during pyrolysis were carried out on a Setsys Evolution16/18 thermal analyzer coupled to an Omni Star mass spectrometer. The TGA was operated from room temperature to 1200 °C at 10 °C /min under a continuous flow of high-purity argon.

3. Results and discussion

3.1 Appearance of the products

Fig. 1 shows a photograph of the disc-shaped silicon-containing pitch-derived carbon materials after pyrolysis at various temperatures. The surface color of the sample obtained by pyrolysis of silicon-containing pitch-derived carbon material at 1200 °C is black, similar to that of the sample before pyrolysis. After pyrolysis at 1300 °C, the surface color of the sample turns from black to gray-green. This change in color indicates that the surface of the sample has been covered by a layer of pyrolysis products. As the pyrolysis temperature increases from 1300 to 1400 °C, the surface color of the sample changes from gray-green to gray-white. Upon increasing the pyrolysis temperature to 1500 °C, the surface color of the sample changes into light green. The change in surface color of the sample may be caused by the variation of the thickness and morphology of the pyrolysis product layer, which is dependent on pyrolysis temperature.

3.2 X-ray diffraction analysis of the products

XRD was performed to understand the product's phase evolution with increasing pyrolysis temperature. Fig. 2a shows the XRD patterns of the top surface of the silicon-containing pitch-derived carbon materials after pyrolysis at various temperatures. It is evident that the XRD pattern of the top surface of the sample obtained at 1200°C displays the characteristics of an amorphous material. Its broad diffraction peak in the 2θ range from 20° to 30° can be attributed to amorphous SiOC glasses and amorphous carbon [14]. After pyrolysis at 1300 °C, three diffraction peaks are observed at $2\theta = 35.6°$, 60.5° and 71.8°, corresponding to the (111), (220) and (311) planes of β-SiC, respectively (JCPDS Card no. 29-1129). The weak diffraction peak at $2\theta = 26.6°$ can be indexed to SiO_2 (JCPDS Card no. 65-0466). This reveals that the gray-green pyrolysis product deposited on the carbon matrix shown in Fig. 1b is composed of β-SiC and traces of SiO_2. As the pyrolysis temperature increases to 1400 °C, the intensity of the β-SiC diffraction peak phase clearly increases, while the diffraction peaks of amorphous SiOC and SiO_2 almost disappear from the XRD pattern of the pyrolysis product. In addition, a low-intensity peak at $2\theta = 33.6$ ° (marked with "SF"), which is usually ascribed to stacking faults within the β-SiC crystals [10], is also observed. Increasing the pyrolysis temperature to 1500 °C results in a further increase in the peak intensity for the β-SiC phase. These changes imply that increasing pyrolysis temperature facilitates the growth of β-SiC crystals. Fig. 2b displays the XRD patterns of the cross-sections of the samples before pyrolysis and after pyrolysis at various temperatures. No obvious Bragg diffractions are detected in the silicon-containing pitch-derived carbon materials before pyrolysis, revealing its amorphous structure. After pyrolysis at 1200 °C for 1 h, the broad diffraction peaks of amorphous SiOC and carbon appear. In addition, three weak diffraction peaks corresponding to β-SiC phase are also observed in its cross-section's XRD pattern. This indicates that β-SiC crystals have been formed in the carbon matrix. It is known that amorphous SiOC glasses are not stable at high temperatures and at temperatures of > 1000 °C-1200 °C, they will undergo a phase separation process, resulting in the formation of SiC nanocrystals and amorphous SiO_2, accompanied by the release of SiO and CO gases [15]. The phase separation process can be described roughly by the following equation (1) [16].

$$5SiOC \rightarrow SiO_2\ (s) + 3SiC\ (s) + SiO\ (g) + 2CO\ (g) \qquad (1)$$

Therefore, the presence of some SiC in the carbon matrix can be attributed to the phase separation process of amorphous SiOC glass. Increasing pyrolysis temperature to 1300°C results in the decrease in intensity of the broad peak corresponding to the amorphous SiOC and carbon phases, concurrently with the increase in the peak intensity of the SiC phase. This can be attributed to the continued phase separation of SiOC and the initiation of the carbo-thermal reduction between amorphous SiO_2 and free carbon above 1200 °C according to the following equation (2) [17].

$$SiO_2\ (s) + 3C\ (s) \rightarrow SiC\ (s) + 2CO\ (g) \qquad (2)$$

Meanwhile, a part of the SiO_2 further reacts with surrounding free carbon to form gaseous SiO and CO according to equation (3) [18].

$$SiO_2(s) + C(s) \rightarrow SiO\ (g) + CO\ (g) \qquad (3)$$

As pyrolysis temperature further increases to 1400 °C and 1500 °C, the phase separation process of amorphous SiOC approaches completion [14], and at the same time the carbo-thermal reduction of SiO_2 is further intensified. As a result, more and more SiC nanocrystals are formed in-situ in the carbon matrix. This leads to the remarkable increase in the intensity of the diffraction peaks assigned to β-SiC phase in the cross-section XRD patterns of the samples obtained at 1400 °C and 1500 °C. Diffraction peaks of crystalline SiO_2 are detected in the sample obtained at 1500 °C and this could be attributed to the crystallization of unreacted amorphous SiO_2 at high temperature.

3.3 SEM/EDX analysis of the products

To determine the microstructure and composition of the pyrolysis products, SEM coupled with EDX was employed. Fig. 3 shows the typical SEM images of the pyrolysis products deposited on the carbon matrix. For the pyrolysis product obtained at 1200 °C, only a small quantity of straight nanowires are formed on the top surface of the carbon matrix. These nanowires show a radiating arrangement and are rooted in several clusters (Fig. 3a). From the high magnification image shown in Fig. 4a, it can be seen that the diameters of the nanowires are in the range of 42-126 nm, the average diameter is 85 nm and the length ranges from 10 to 50 microns. Individual nanowires have uniform diameter along their entire length. No spherical caps are observed on the tips of the nanowires. The EDX analysis (shown in Fig. 4e) indicates that these nanowires are mainly composed of Si and C. The atomic ratio of Si/C of the nanowires is close to 1, which corresponds to the stoichiometric composition of SiC, indicating the formation of SiC nanowires without catalytic assistance. Unlike the nanowires, the EDX spectrum of the carbon matrix (shown in Fig. 4f) confirms the presence of Si, C and O, which is consistent with the XRD analysis in Fig. 2a. As the pyrolysis temperature increases to 1300 °C, a large quantity of straight (and some curved) nanowires have been formed and are randomly oriented. These nanowires have grown into an extensive network that hides the carbon matrix (shown in Fig. 3b). As can be seen from the high magnification SEM image of the nanowires synthesized at 1300 °C (shown in Fig. 4b), the average diameter is about118 nm, and the length ranges from tens to hundreds of micrometers. Both increase compared with those of the product synthesized at 1200 °C. In addition, it is also found that the nanowires synthesized at 1300 °C have a smooth and clean surface and no particles are attached to their surfaces. Most of nanowires have a very interesting bamboo-like morphology with a stem-node structure (see the inset in Fig. 4b), which is quite different that of the nanowires synthesized at 1200 °C. Figure 3c is a typical SEM image of the pyrolysis product obtained at 1400 °C, showing that relatively high-density nanowires have grown homogeneously on the top surface of the carbon matrix. As can be seen from Fig. 4c, most of the nanowires synthesized at 1400 °C are straight and present a uniform diameter along their length direction. The average diameter of the nanowire increases to 183 nm with the increase of pyrolysis temperature. Very interestingly, a coiled nanowire is found amongst the straight nanowires, as indicated by an arrow. According to Yang’s work [19], such curved growth results from a fluctuation of the kinetic growth condition, which disturbs the balance between growth along different directions. The inset in Fig. 4c shows the typical tip morphology of these synthesized nanowires. It can be seen that the tip presents a hexagonal terrace, roughly analogous to the morphology reported in the literature [20]. This morphology is considered to result from screw dislocation growth. Further increasing the pyrolysis temperature to 1500 °C results in the formation of a large quantity of irregular agglomerates dispersed within the nanowire network, as shown in Figs. 3d and 4d. The EDX analysis in Fig. 4g reveals that the agglomerates contain Si and C. Combined with the XRD analysis in Fig. 2a, the agglomerates can be identified as SiC grains. The formation of SiC agglomerates may be associated with the higher reaction rate resulting from the higher pyrolysis temperature. The high magnification image shown in Fig. 4d reveals that almost all of the nanowires are straight and have a slightly fluctuating diameter of about 220 nm, which is much larger than that of the nanowires synthesized at 1400 °C. Moreover, the bamboo-like morphology of the nanowires synthesized at 1500 °C is very similar to that of the nanowires synthesized at 1300 °C. The SEM observation indicates that pyrolysis temperature has an important influence on the growth the SiC nanowires, which is reflected by the variations in amount, length, diameter and morphology of the nanowires. In order to understand the growth mechanism of the SiC nanowires, products from pyrolysis of pure PCS at different temperatures were also studied by SEM. However, in this case, only black SiC foam ceramic was obtained in the temperature range of 1200-1500 °C. These results indicate that the coal tar pitch is definitively required for the synthesis of the SiC nanowires.

3.4 TEM/HRTEM/SAED analysis of the products

TEM, HRTEM and SAED were also carried out to further characterize the morphology and detailed crystalline structure of the synthesized nanowires. Figs. 5a-5c show the TEM and HRTEM images of the nanowires synthesized at 1400 °C. From the typical low-magnification TEM image shown in Fig. 5a, it can be seen that these nanowires are not uniform in diameter. Figure 5b is a typical HRTEM image of a single nanowire with a cone-shaped tip. The HRTEM image reveals that the stem of the nanowire has alternate bright and dark striations along the growth direction. The high-density of striations means that there are numerous stacking faults perpendicular to the nanowire’s longitudinal axis. The formation of stacking faults is generally considered to be attributed to the change of stacking sequences under the fluctuation of kinetic growth condition [17], and it thermodynamically favors decreasing the total free energy of the nanowires. Thus, the formation of stacking faults enhances the growth of the SiC nanowires. Surprisingly, no striations can be found at the tip of the nanowire. The high magnification TEM image shown in Fig. 5c indicates that the tip of the nanowire has regularly arrayed fringes and the inter-planar spacing between two adjacent lattice fringes is 0.25 nm, which is precisely equal to the inter-planar distance between the (111) planes in a β-SiC crystal. This implies that the nanowires have grown on the (111) plane along the [111] direction, which agrees well with the strongest diffraction peak, corresponding to the (111) plane of β-SiC, in the XRD patterns (Fig. 2a). It is well known that the surface energy of (111) plane is lower than that of any other plane for a β-SiC crystal. Therefore, growing along the direction perpendicular to the (111) plane can facilitate a remarkable reduction in the system’s energy [21].The upper-right inset in Fig. 5b is the SAED pattern taken from the tip of the nanowire. The sharp spots in the SAED pattern indicate that the tip of the nanowire has a perfect single crystalline structure. The SAED pattern also further confirms that the growth direction of β-SiC nanowires is parallel to the [111] direction. In contrast to the tip of the nanowire, dense stacking faults along the [111] direction are clearly observed in the stem region of the nanowire. The corresponding SAED pattern (see lower-left inset in Fig. 5b) shows bright spots and diffuse streaks, which are typically characteristic of single crystals containing stacking faults [11, 22]. Figs. 5d-5f show the TEM and HRTEM images of an individual bamboo-like SiC nanowire synthesized at 1500°C. As can be seen from the typical low magnification TEM image shown in Fig. 5d, the nanowire exhibits a smooth stem-node structure. The nodes, with larger diameter, grow along the entire length of the bamboo-like SiC nanowire, and the distance between two adjacent nodes shows a non-periodic variation. From the SAED pattern and HRTEM image of the node of the nanowire (shown in Fig. 5d and 5e), the nodes of the bamboo-like nanowire are composed of single crystalline β-SiC without stacking faults and twins. However, many twins are found in the HRTEM image of the stem of the nanowire (shown in Fig. 5f). The corresponding SAED pattern in the inset of Fig. 5d also confirms the existence of the twins. Unlike the stacking faults, the presence of twins has a close relationship with the large stress generated in the nanowires, which is mainly caused by the difference in the surface energy of the (111) facet of Si and C [9].The large internal stress could drive the formation of twins along the growth direction of the SiC nanowires. All these results suggest that many crystal defects (i.e. stacking faults and twins) exist in the synthesized SiC nanowires which are associated with different morphologies. Moreover, it is also observed in Fig. 5c that the SiC nanowire is covered with a continuous amorphous layer with a thickness of 1-2 nm. Fig. 5g is the EDX spectrum from the area within the circle drawn on the nanowire in Fig. 5c. It reveals that this coating is composed of C, Si and a small amount of O. The EDX analysis, combined with XRD analysis in Fig. 2a indicates that the coating is amorphous SiO_2. A similar phenomenon has also been reported by Dai et al. [23]. The SiO_2 coating is believed to be formed on the surface of the SiC nanowires during the cooling stage via the following reaction (4) [24].

$$3SiO(g) + CO(g) \rightarrow SiC\,(s) + 2SiO_2\,(s) \qquad (4)$$

In this study, the gaseous SiO and CO are believed to be mainly derived from the decomposition of the amorphous SiOC glass and/or carbo-thermal reduction of SiO_2 during pyrolysis of silicon-containing pitch-based carbon materials.

3.5 FTIR analysis of the products

In order to achieve more insight into the formation process of the SiC nanowires, the structure of TSCTP, PCS and products from pyrolysis of their hybrid precursor at various temperatures were characterized by FTIR spectrometry. As shown in Fig. 6, the observed peaks are in the typical regions for characteristic chemical bonds and can be helpful in identification of the starting compounds as well as intermediate and final products. In the case of TSCTP, the absorption peak at 3040 cm^{-1} is attributed to the aromatic C–H stretching vibration, while the absorption peaks between 3000 cm^{-1} and 2800 cm^{-1} are ascribed to the aliphatic C–H stretching vibration. The peaks at 1600 cm^{-1}, 1440 cm^{-1} and 745 cm^{-1} correspond to the aromatic C=C stretching vibration, C–H in-plane bending vibration and C–H out-of-plane bending vibration, respectively. The spectrum of PCS shows a strong absorption at about 2100 cm^{-1}, which is assigned to the Si–H stretching vibration. The peaks at about 1250 cm^{-1} and 830 cm^{-1} are typical of the Si–C stretching vibration in ≡Si–CH_3 and that at about 1024 cm$^{−1}$ of the –CH_2– in the –Si–CH_2–Si– wagging vibration [25]. The spectrum for the 350 °C-homogenized mixtures are best described as the composite spectra of the two components' contributions. For the pyrolysis product at 900 °C, the most remarkable change is the disappearance of the Si–H stretching vibration peak at 2100 cm$^{−1}$ and the simultaneous appearance of two new peaks at about 1089 cm$^{−1}$ and 460 cm^{-1}, which correspond to Si–O stretching vibration and Si–O–Si rocking vibration, respectively [18]. This change could result from reactions of the ≡Si–H in the PCS with hydroxyl-containing species in TSCTP according to the following H_2-elimination reaction (5).

$$\equiv\text{Si–H} + \text{–OH} \rightarrow \equiv\text{Si–O–} + H_2 \qquad (5)$$

The presence of –OH groups in TSCTP is evidenced by its broad peak at 3200–3600 cm$^{−1}$. Additionally, it is also found that the peaks associated with the C–H and ≡Si–CH_3 functional groups almost disappear, which could be related to the formation of amorphous SiOC glass in carbon matrix and the simultaneous escape of CH_4. As the pyrolysis temperature increases to 1200 °C, the peak at about 1600 cm$^{−1}$ corresponding to the aromatic C=C stretching vibration disappears, and a new weak peak at around 810 cm^{-1} associated with Si–C stretching occurs, implying the formation of an Si-C structure in carbon matrix. In addition, the peak associated with Si–O stretching vibration noticeably both broadens and increases in intensity. These changes in absorbance peaks agree well with the XRD results in Fig. 2b, and thus further confirm that the phase separation process of amorphous SiOC glass starts at temperatures of > 1000 °C-1200 °C. As the pyrolysis temperature increases to 1300 °C, the peak corresponding to Si-C stretching vibration clearly increases in intensity, whereas the intensity of Si–O stretching vibration peak decreases significantly. These variations are caused by the continuous phase separation of SiOC and the coincident carbo-thermal reduction of the Si–O bond. Increasing pyrolysis temperature to 1400 °C and 1500 °C results in a further increase in the intensity of the Si–C stretching vibration peak and the near disappearance of the Si–O stretching vibration peak, accompanied with the occurrence of a shoulder peak at about 970 cm^{-1}. This FTIR analysis, combined with the XRD results in Fig. 2b reveals that most of the amorphous SiO_2 transforms into crystalline β-SiC via carbo-thermal reduction reaction during pyrolysis at 1400-1500 °C.

3.6 TG-MS analysis of gaseous products released during pyrolysis

A system coupling TG with MS was used in this study to further investigate the volatile species generated during pyrolysis of the silicon-containing pitch-derived carbon materials. In the TG-MS system, the volatile species are identified by their molecular masses corresponding to mass number (m/z) signal. The intensity of the m/z signal in this technique is related to the amount of the volatile species. Fig. 7 presents the sample weight loss and the intensity of m/z signals detected in the MS versus pyrolysis temperature. The silicon-containing pitch-derived carbon material shows a weight loss of about 4 wt% during pyrolysis from room temperature to 1200 °C, as can be seen from the TGA curve in Fig. 7. The major gaseous products evolved are identified as H_2O, CO, CH_4 and SiO. Water vapor is the dominant volatile and is released at a broad range of temperatures from room temperature to 1200 °C. This is believed to arise from volatilization of physically adsorbed water at low temperatures and the precursor deoxygenation reaction during pyrolysis at high temperatures. CO is the next most abundant product and its evolution below 1000 °C is likely to be caused by the deoxygenation reaction of the pitch-derived carbon matrix during pyrolysis. When pyrolysis temperature is above 1000 °C, the rate of CO generation increases noticeably. Unlike CO, the evolution of CH_4 is related to the dehydrogenation reaction during pyrolysis and its generation rate is relatively constant over the wide temperature range from room temperature to 1200 °C. The emission of SiO starts at about 1000 °C and the generation rates of SiO and CO increase drastically when pyrolysis temperature increases to about 1100 °C, which could be mainly attributed to onset of the phase separation process of the amorphous SiOC glass. In addition, traces of H_2 gas are also detected in the evolved mixture. The generation of H_2 gas is probably related with the reaction between water vapor and solid carbon.

3.7 Growth mechanism of the SiC nanowires

The above characterization indicates that the pyrolysis temperature has significant influence on the formation and growth of β-SiC nanowires. In most cases, the growth of SiC nanowires can be explained by the widely accepted vapor-liquid-solid (VLS) mechanism [26] or vapor-solid (VS) mechanism [27], which are dependent on the environmental conditions during growth. Generally, the growth of nanowires with the assistance of a metal catalyst follows the VLS mechanism. In this case, the typical structure involves a metallic droplet sitting on the tip of each nanowire. However, in the present work, no droplets are found on the tips of the nanowire. This indicates that the growth of the as-prepared SiC nanowires does not follow the VLS mechanism. Instead, the VS mechanism may dominate during the growth of the SiC nanowires. In order to better understand the growth mechanism of the SiC nanowires synthesized in this work, the major steps proposed for the formation of SiC nanowires are schematically illustrated in Fig. 8. In essence, the formation of nanowires can be divided into two stages: nucleation and growth. The SiC nanocrystals derived from the phase separation process of amorphous SiOC glass and/or carbo-thermal reduction of SiO_2 during the pyrolysis of the silicon-containing pitch-derived carbon matrix are believed to act as the nuclei in this mechanism. Another prerequisite for the formation of the SiC nanowires is an adequate supply of active substance in the growth stage. In this work, gaseous SiO, CO and CH_4 act as the active substance. SiO gas supplies Si source for the growth of SiC nanowires, and most of them are released via phase separation and/or carbo-thermal reduction during pyrolysis. Besides, according to the report from X. Li et al [28], a small amount of CH_4 and H_2 generated during pyrolysis can also react with SiO_2 to form SiO via the following reactions (6) and (7), respectively. The active substance CO and CH_4 provide C source for the growth of SiC nanowires, which can react with SiO to produce SiC by the following reactions (8) and (9), respectively.

$$SiO_2\,(s) + CH_4\,(g) \rightarrow SiO\,(g) + CO\,(g) + 2H_2\,(g) \qquad (6)$$

$$SiO_2 (s) + H_2 (g) \rightarrow SiO (g) + H_2O (g) \qquad (7)$$

$$SiO (g) + 3CO (g) \rightarrow SiC (s) + 2CO_2 (g) \qquad (8)$$

$$SiO (g) + 2CH_4 (g) \rightarrow SiC (s) + CO (g) + 4H_2 (g) \qquad (9)$$

The resulting H_2O (reaction (7)) and CO_2 (reaction (8)) immediately react with the surrounding free carbon to form CO according to the following reactions (10) and (11), respectively. The free carbon also reacts with the resulting H_2 (reactions (6) and (9)) to form CH_4 via the following reaction (12). These reactions provide sustainable C source for the growth of SiC nanowires.

$$H_2O (g) + C (s) \rightarrow H_2 (g) + CO (g) \qquad (10)$$

$$CO_2 (g) + C (s) \rightarrow CO (g) \qquad (11)$$

$$2H_2 (g) + C (s) \rightarrow CH_4 (g) \qquad (12)$$

As shown in Fig. 8a, the pyrolysis of the silicon-containing pitch-derived carbon matrix was carried out in a closed graphite crucible. When the pyrolysis temperature reaches about 1100 °C, phase separation of the amorphous SiOC glass is initiated and this results in the formation of a small quantity of SiC nanocrystals. Meanwhile, gaseous SiO, CO, H_2O, CH_4 and H_2 are generated, as illustrated in Fig. 8b. At this point, theoretically, the two prerequisites for the formation of nanowires have been fulfilled. However, in practice there is as yet no nanowire formation on the surface of pitch-derived carbon matrix. This is probably related to insufficient concentration of gaseous SiO, CO and CH_4. As the pyrolysis temperature increases to 1200 °C, the concentrations of gaseous SiO, CO and CH_4 increase to a critical level and trigger the growth of SiC nanowires. Thereafter, SiO, CO and CH_4 in the head-space of the closed graphite crucible continuously diffuse toward the as-formed SiC nuclei and then react to produce SiC there via the VS mechanism, as shown in Fig. 8c. The oriented growth as well as continuous generation and reaction of SiO, CO and CH_4 are responsible for the formation of SiC nanowires. The formation of low-density SiC nanowires at 1200 °C can be attributed to the relative scarcity of nuclei and the relatively lower concentration of SiO, CO and CH_4, which are dependent on the pyrolysis temperature. Increasing pyrolysis temperature to 1300-1500 °C accelerates the phase separation of amorphous SiOC glass and, more importantly, the carbo-thermal reduction reaction between SiO_2 and free C is triggered and gradually intensifies. As a result, both the number of SiC nuclei and the concentration of evolved SiO and CO gases increase significantly. These two key factors facilitate the growth and formation of high-density SiC nanowires on the top surface of the carbon matrix in the temperature range of 1300 -1500 °C (as illustrated in Fig. 8d). Especially worthy of mention are the many SiC agglomerates that are found in the SiC nanowire network when pyrolysis temperature increases to 1500 °C. This high pyrolysis temperature not only leads to excessive concentration of the gaseous SiO and CO, but also enhances the driving force of reactions (8) and (9). Both promote SiC crystal growth in several directions and the formation of SiC agglomerates. In addition, the pitch-derived carbon matrix plays an important role in reactions (2), (3), (10), (11) and (12), which facilitate the nucleation and growth of SiC nanowires. This explains clearly why only black SiC foam ceramic was obtained when no coal tar pitch was employed.

4. Conclusions

A simple and convenient method was developed for the synthesis of SiC nanowires on a large scale based on precursor pyrolysis, where PCS and TSCTP were used as raw materials. The main conclusions are summarized as follows:

(1) Pyrolysis temperature has an important influence on the formation of SiC nanowires. The growth of the SiC nanowires starts at around 1200 °C, and a large quantity of nanowires are formed at 1300-1500 °C. These SiC nanowires have average diameter in the range of 85–220 nm and length ranging from tens to hundreds of micrometers. Increasing the pyrolysis temperature results in an increase in the average diameter and in the quantity of nanowires produced. The typical morphology of the nanowires also changes with the variation of pyrolysis temperature.

(2) The synthesized SiC nanowires have single-crystalline structure and grow along the [111] direction. There also exist numerous stacking faults and twins perpendicular to the growth direction.

(3) The formation of the SiC nanowires may be dominated by the VS mechanism, where SiC nanocrystals act as nuclei and gaseous SiO, CO and CH_4 act as active substance. The nuclei originate from the phase separation of amorphous SiOC glass and/or the reduction of SiO_2 by free carbon during pyrolysis.

The success of synthesis of SiC nanowires in a pitch-based carbon matrix opens new opportunities for the further preparation of nanowire-reinforced C/C composites with improved mechanical properties.

Acknowledgements

The authors acknowledge the financial support of the Key Program of Major Research Plan of the National Natural Science Foundation of China (Grant no. 91016003), and the Special Fund of the National Natural Science Foundation of China (Grant no. 51352001).

Reference

[1] Z. Lei, Q.G. Fu, T.Y. Liu, B.Y. Tan, In-situ PIP-SiC NWs-toughened $SiC-CrSi_2-Cr_3C_2-MoSi_2-Mo_2C$ coating for oxidation protection of carbon/carbon composites, J. Alloys Compd. 675 (2016) 348–354.

[2] R.B. Wu, K. Zhou, X.K. Qian, Y.Z. Huang, Well-aligned SiC nanoneedle arrays for excellent field emitters, Mater. Lett. 91 (2013) 220–223.

[3] C.O. Jang, T.H. Kim, S.Y. Lee, D.J. Kim, S.K. Lee, Low-resistance ohmic contacts to SiC nanowires and their applications to field-effect transistors, Nanotechno. 19 (2008) 13304–13309.

[4] J. Li, T. Shirai, M. Fuji, Rapid carbothermal synthesis of nanostructured silicon carbide particles and whiskers from rice husk by microwave heating method, Adv. Powder. Technol. 24 (2013) 838–843.

[5] W.Q. Han, P. Redlich, F. Ernst, M. Rühle, Synthesizing boron nitride nanotubes filled with SiC nanowires by using carbon nanotubes as templates, Appl. Phys. Lett. 75 (1999) 1875–1877.

[6] Q.H. Wang, Y.W. Li, S.L. Jin, S.B. Sang, Catalyst-free hybridization of silicon carbide whiskers and expanded graphite by vapor deposition method, Ceram. Int. 41 (2015) 14359–14366.

[7] G. Shen, D. Chen, K.B. Tang, Y.T. Qian, S.Y. Zhang, Silicon carbide hollow nanospheres, nanowires and coaxial nanowires, Chem. Phys. Lett. 3751 (2003) 177–184.

[8] W.Y. Yang, Z.P. Xie, J.J. Li, H.Z. Miao, L.G. Zhang, L.N. An, Ultra-long single-crystalline α-Si_3N_4, nanowires: derived from a polymeric precursor, J. Am. Ceram. Soc. 88 (2005) 1647–1650.

[9] M. Lodhe, A. Selvam, A. Udayakumar, M. Balasubramanian, Effect of polycarbosilane addition to a mixture of rice husk and coconut shell on SiC whisker growth, Ceram. Int. 42 (2016) 2393–2401.

[10] J.M. Pan, Q.B. Lu, X.N. Cheng, X.H. Yan, C.H. Zhang, Large-scale synthesis of SiC nanowires from polysiloxane and wood powder composites, Cryst. Res. Technol, 47 (2012) 1237–1242.

[11] K.F. Cai, Q. Lei, A.X. Zhang, A simple route to ultra long SiC nanowires. J. Nanosci & Nanotechno, 7(2007) 580–583.

[12] C. Vakifahmetoglu, E. Pippel, J. Woltersdorf, P. Colombo, Growth of one-dimensional nanostructures in porous polymer-derived ceramics by

catalyst-assisted pyrolysis. Part I: iron catalyst, J. Am. Ceram. Soc. 93 (2010) 3709–3719.

[13] M. Adam, C. Vakifahmetoglu, P. Colombo, M. Wilhelm, G. Grathwohl, Polysiloxane-derived ceramics containing nanowires with catalytically active tips, J. Am. Ceram. Soc. 97 (2014) 959–966.

[14] G.D. Sorarù, S. Modena, E. Guadagnino, P. Colombo，J. Egan, C. Pantano, Chemical durability of silicon oxycarbide glasses, J. Am. Ceram. Soc, 85 (2002) 1529–1536.

[15] H.J. Kleebe, C. Turquat, G.D. Sorarù, Phase separation in an SiCO glass studied by transmission electron microscopy and electron energy-loss spectroscopy, J Am Ceram Soc. 84 **(**2001) 1073–1080.

[16] Q.S. Ma, Z.H. Chen, W.W. Zheng, H.F. Hu, Cross-linking and pyrolysis of polysiloxane/divinylbenzene, Journal of National University of Defense Technology. 23 (5) (2001) 40–44.

[17] F. Li, G. Wen, L. Song, Growth of nanowires from annealing SiBONC nanopowders. J. Cryst.Growth. 290 (2006) 466–472.

[18] Y. Chen, C.G. Wang, B. Zhu, Y.X. Wang, Y.Z. Liu, T.T. Tan, R.R. Gao, X. Lin, F. Meng, Growth of SiC whiskers from hydrogen silicone oil, J. Cryst. Growth. 357 (2012) 42–47.

[19] W. Yang, H. Araki, Q.L. Hu, N. Ishikawa, H. Suzuki, T. Noda, In situ growth of SiC nanowires on RS-SiC substrate, J. Cryst. Growth. 264 (2004) 278–283.

[20] J.J. Chen, Y. Pan, R.B. Wu. Growth mechanism of twinned SiC nanowires

synthesized by a simple thermal evaporation method. Physica. E. 42 (2010) 2335–2340.

[21] S.M. Zhu, H.A. Xi, Q. Li, R.D. Wang, In situ growth of β-SiC nanowires in porous SiC ceramics, J. Am. Ceram. Soc. 88 (2005) 2619–2621.

[22] Y.S. Liu, J. Men, W. Feng, Catalyst-free growth of SiC nanowires in a porous graphite substrate by low pressure chemical vapor infiltration, Ceram. Int. 40 (2014) 11889–11897.

[23] J.X. Dai, J.J. Sha, Z.F. Zhang, Y.C. Wang, W. Krenkel. Synthesis of high crystalline beta SiC nanowires on a large scale without catalyst, Ceram. Int. 41 (2015) 9637–9641.

[24] X.W. Du, X. Zhao, S.L. Jia, Y.W. Lu, J.J. Li, N.Q. Zhao, Direct synthesis of SiC nanowires by multiple reaction VS growth, Mater. Sci. Eng. 136 (2007) 72–77.

[25] Y.L. Li, E. Kroke, R. Riedel, F. Babonneau, Thermal cross-linking and pyrolytic conversion of poly(ureamethylvinyl)silazanes to silicon-based ceramics, Appl. Organomet Chem. 15 (2001) 820–832.

[26] Y.J. Hao, J.B. Wagner, D.S. Su, G.Q. Jin, X.Y. Guo, Beaded silicon carbide nanochains via carbothermal reduction of carbonaceous silica xerogel, Nanotechno. 17 (2006) 2870–2874.

[27] Y.H. Gao, Y. Bando, K. Kurashima, T. Sato, SiC nanorods prepared from SiO and activated carbon, J. Mater. Sci. 37 (2002) 2023–2029.

[28] X. Li, G.Q. Zhang, R. Tronstad, O. Ostrovski, Synthesis of SiC whiskers by VLS and VS process, Ceram. Int. 42 (2016) 5668-5676.

Table and Figure captions

Fig. 1 Disc-shaped silicon-containing pitch-derived carbon materials after pyrolysis at various temperatures: (a) 1200 °C, (b) 1300 °C, (c) 1400 °C and (d) 1500 °C

Fig. 2 XRD patterns of the top surface (a) and the cross-section (b) of the silicon-containing pitch-derived carbon materials before pyrolysis and after pyrolysis at various temperatures

Fig. 3 Low magnification SEM images of the SiC nanowires synthesized by pyrolysis of silicon-containing pitch-derived carbon materials at various temperatures (a:

1200 °C; b: 1300 °C; c: 1400 °C; and d: 1500 °C)

Fig. 4 High magnification SEM images the SiC nanowires synthesized by pyrolysis of silicon-containing pitch-derived carbon materials at various temperatures (a: 1200 °C; b: 1300 °C; c: 1400 °C; and d: 1500 °C) and EDX analysis of various locations in Fig.4a and d. The insets in Fig. 4b and c show the typical morphology of the nanowires synthesized at 1300 °C and 1400 °C

Fig. 5 (a) A typical low magnification TEM image of the SiC nanowires synthesized at 1400 °C; (b) a typical HRTEM image of a single nanowire with a cone-shaped tip in Fig. 5 (a). The upper-right and lower-left insets are the selected area electron patterns recorded on the cone-shaped tip and the stem of the nanowire, respectively; (c) a magnified HRTEM image of the SiC nanowire with a cone-shaped tip in Fig. 5 (b); (d) a typical low magnification TEM image of the bamboo-like SiC nanowires synthesized at 1500°C. The upper-left and lower-right insets are the selected area electron patterns recorded on the node and the stem of the nanowire, respectively; (e) HRTEM image of a node on the nanowire in Fig. 5 (d); (f) HRTEM image of the stem of the nanowire in Fig. 5 (d); (g) EDX spectrum from the area within the circle drawn on the nanowire in Fig. 5c

Fig. 6 FTIR spectra of the TSCTP, PCS and pyrolysis products obtained by pyrolysis of the hybrid precursor of TSCTP and PCS at various temperatures

Fig. 7 Online coupled TG-MS analysis of gaseous products released during pyrolysis of the silicon-containing pitch-derived carbon materials

Fig. 8 Schematic illustration showing the nucleation and growth of SiC nanowires on the top surface of the silicon-containing pitch-derived carbon matrix via the VS mechanism during pyrolysis in a closed graphite crucible. (a) silicon-containing pitch-derived carbon matrix at the start of pyrolysis; (b) formation of SiC crystal nuclei in the carbon matrix at about 1100 °C; (c) formation of low-density SiC nanowires on the top surface of the carbon matrix at 1200 °C; (d) formation of high-density SiC nanowires on the top surface of the carbon matrix in the temperature range of 1300-1500 °C

Table 1 Properties of the coal tar pitch used in this study

SP[a](°C)	CV[b](wt.%)	TI[c](wt.%)	QI[d](wt.%)
85-90	≥48	≥18	≤0.5

[a] Softening point. [b] Coking value. [c] Toluene insolubles. [d] Quinoline insolubles.

Table 2 Properties of the polycarbosilane in this study

SP[a](°C)	MW[b](u)	CY[c](wt.%)
190-210	20000	64

[a] Softening point. [b] Molecular weight. [c] Ceramic yield

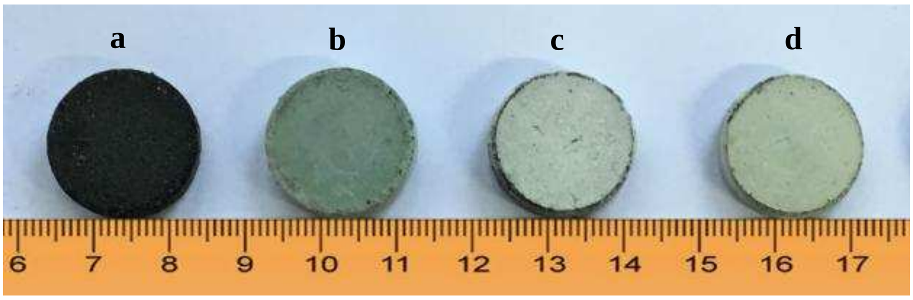

Fig. 1 Disc-shaped silicon-containing pitch-derived carbon materials after pyrolysis at various temperatures: (a) 1200 °C, (b) 1300 °C, (c) 1400 °C and (d) 1500 °C

Figure 2

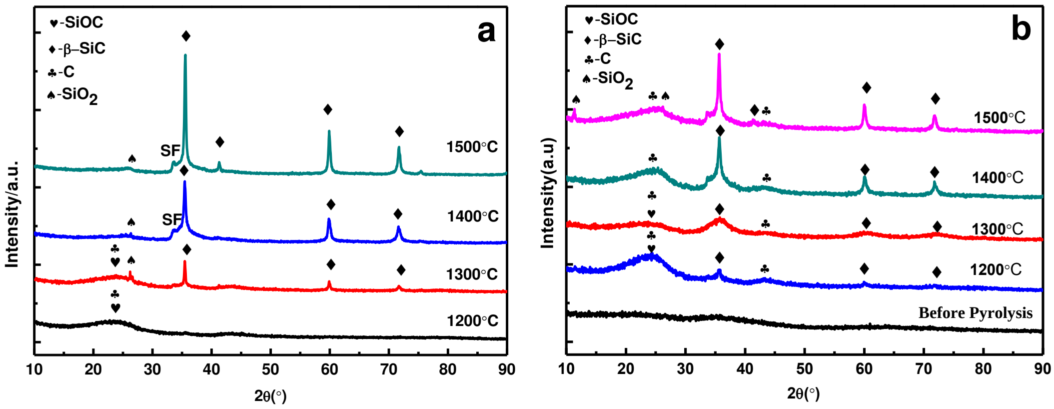

Fig. 2 XRD patterns of the top surface (a) and the cross-section (b) of the silicon-containing pitch-derived carbon materials before pyrolysis and after pyrolysis at various temperatures

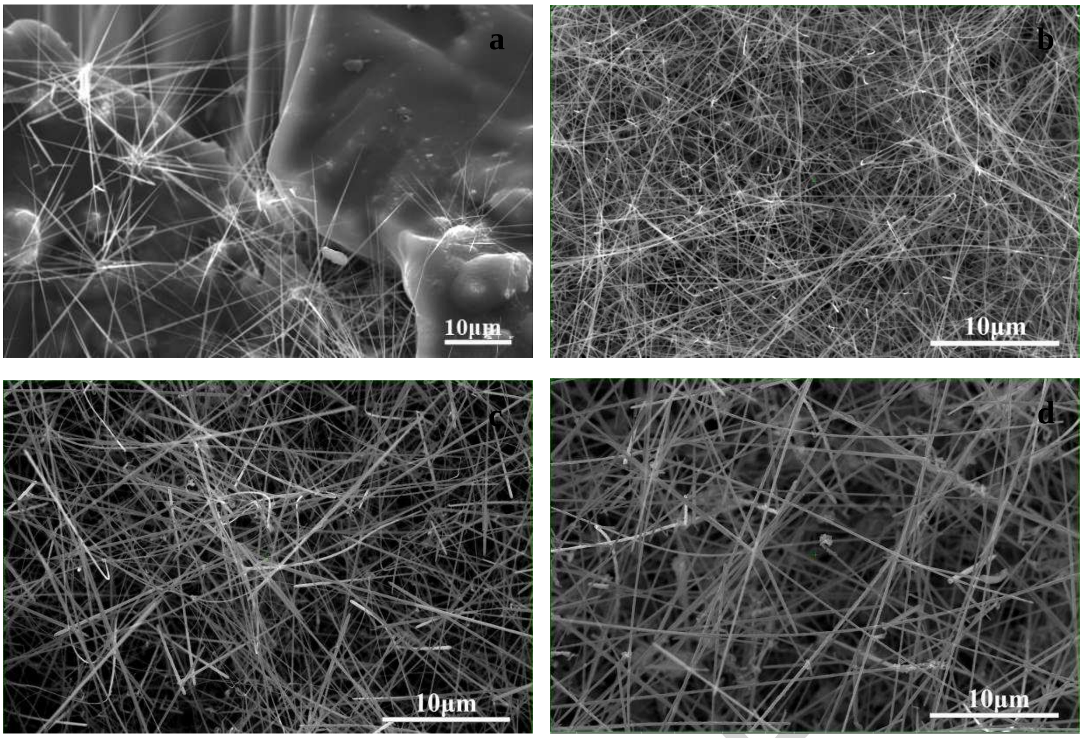

Fig. 3 Low magnification SEM images of the SiC nanowires synthesized by pyrolysis of silicon-containing pitch-derived carbon materials at various temperatures (a: 1200 °C; b: 1300 °C; c: 1400 °C; and d: 1500 °C)

Figure 4

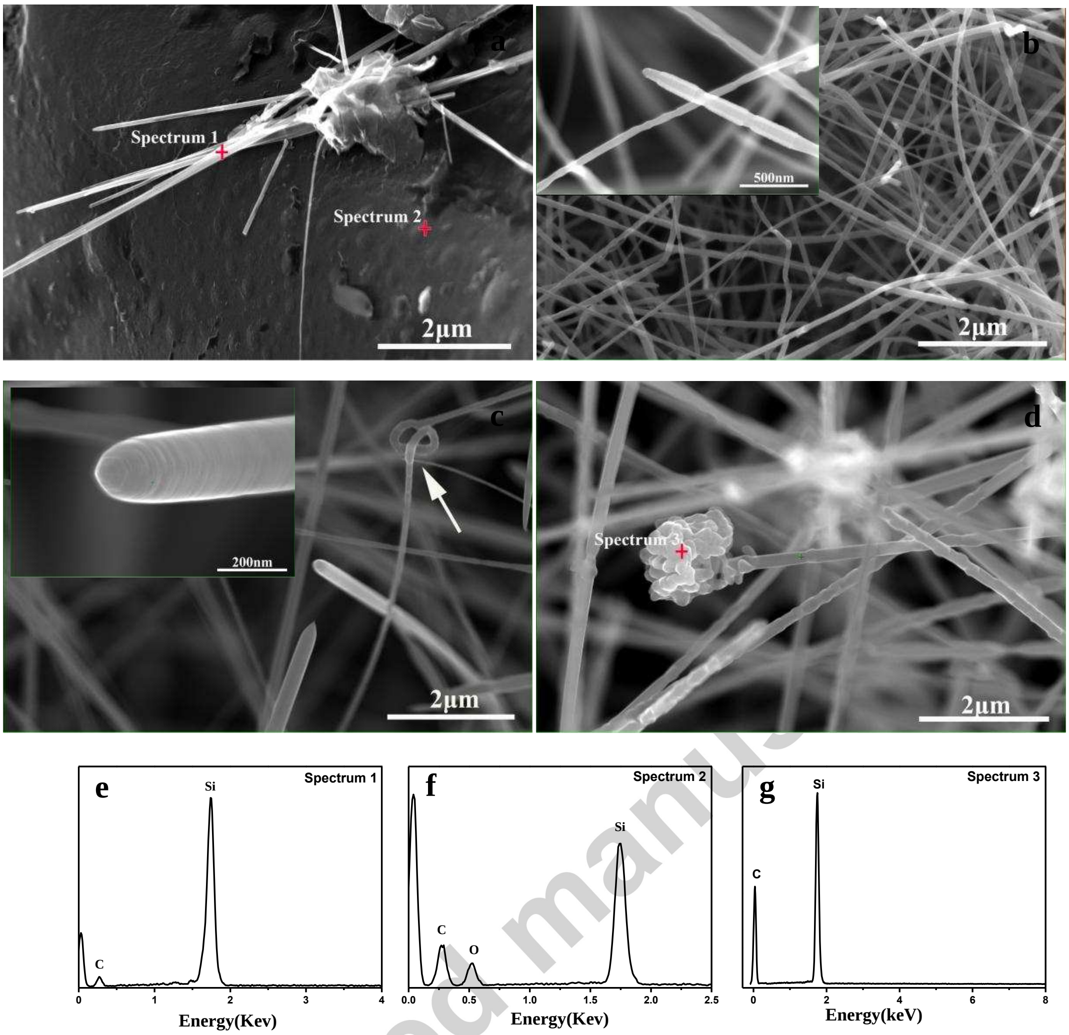

Fig. 4 High magnification SEM images the SiC nanowires synthesized by pyrolysis of silicon-containing pitch-derived carbon materials at various temperatures (a: 1200 °C; b: 1300 °C; c: 1400 °C; and d: 1500 °C) and EDX analysis of various locations in Fig.4a and d. The insets in Fig. 4b and c show the typical morphology of the nanowires synthesized at 1300 °C and 1400 °C

Figure 5

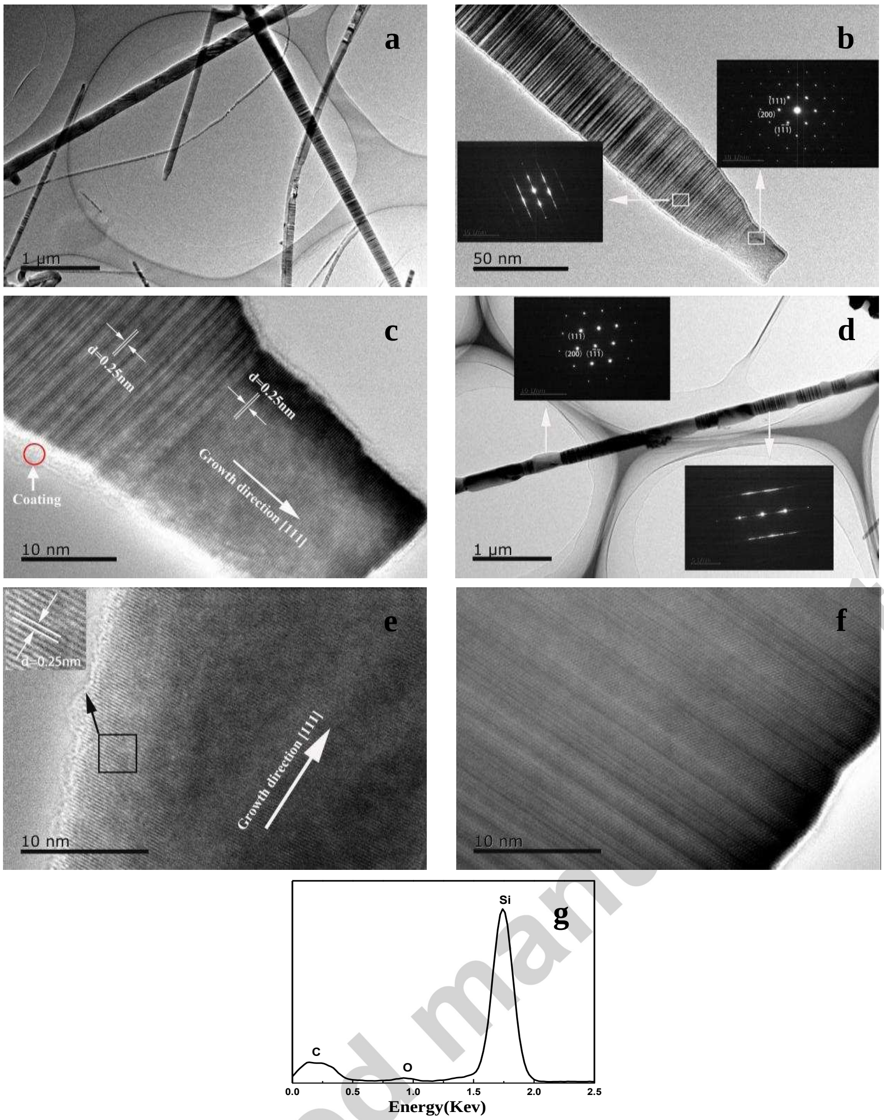

Fig. 5 (a) A typical low magnification TEM image of the SiC nanowires synthesized at 1400 °C; (b) a typical HRTEM image of a single nanowire with a cone-shaped tip in Fig. 5 (a). The upper-right and lower-left insets are the selected area electron patterns recorded on the cone-shaped tip and the stem of the nanowire, respectively; (c) a magnified HRTEM image of the SiC nanowire with a cone-shaped tip in Fig. 5 (b); (d) a typical low magnification TEM image of the bamboo-like SiC nanowires synthesized at 1500°C. The upper-left and lower-right insets are the selected area electron patterns recorded on the node and the stem of the nanowire, respectively; (e) HRTEM image of a node on the nanowire in Fig. 5 (d); (f) HRTEM image of the stem of the nanowire in Fig. 5 (d); (g) EDX spectrum from the area within the circle drawn on the nanowire in Fig. 5c

Figure 6

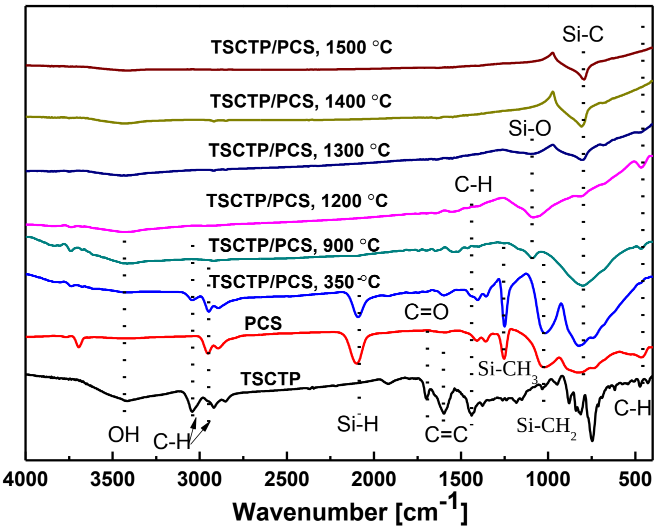

Fig. 6 FTIR spectra of the TSCTP, PCS and pyrolysis products obtained by pyrolysis of the hybrid precursor of TSCTP and PCS at various temperatures

Figure 7

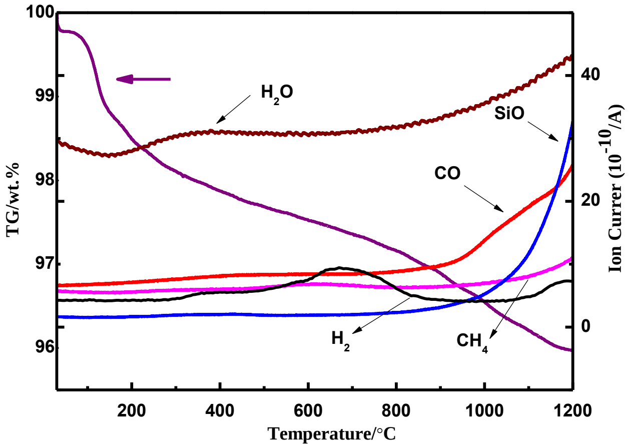

Fig. 7 Online coupled TG-MS analysis of gaseous products released during pyrolysis of the silicon-containing pitch-derived carbon materials

Figure 8

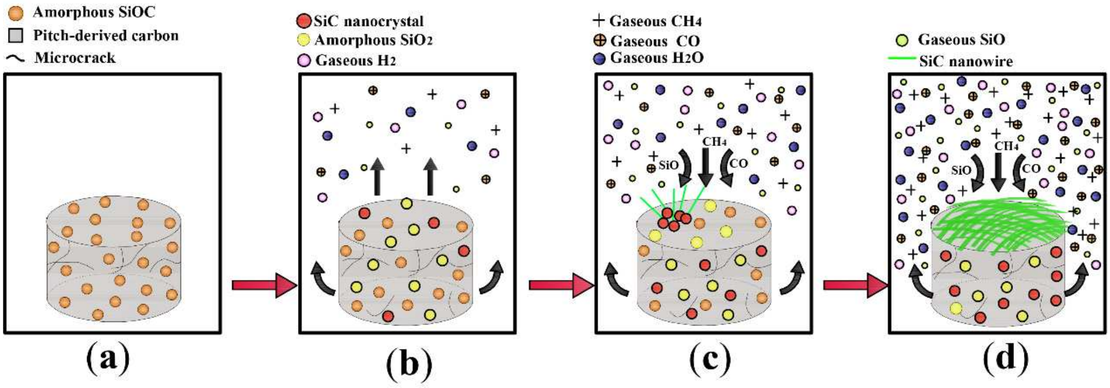

Fig. 8 Schematic illustration showing the nucleation and growth of SiC nanowires on the top surface of the silicon-containing pitch-derived carbon matrix via the VS mechanism during pyrolysis in a closed graphite crucible. (a) silicon-containing pitch-derived carbon matrix at the start of pyrolysis; (b) formation of SiC crystal nuclei in the carbon matrix at about 1100 °C; (c) formation of low-density SiC nanowires on the top surface of the carbon matrix at 1200 °C; (d) formation of high-density SiC nanowires on the top surface of the carbon matrix in the temperature range of 1300-1500 °C